



HAL
open science

SELECTIVE PROPERTIES OF ROUGH SPUTTERED FILMS

G. Harding, S. Craig, P. Curmi, M. Lake

► **To cite this version:**

G. Harding, S. Craig, P. Curmi, M. Lake. SELECTIVE PROPERTIES OF ROUGH SPUTTERED FILMS. Journal de Physique Colloques, 1981, 42 (C1), pp.C1-87-C1-103. 10.1051/jphyscol:1981106 . jpa-00220656

HAL Id: jpa-00220656

<https://hal.science/jpa-00220656>

Submitted on 4 Feb 2008

HAL is a multi-disciplinary open access archive for the deposit and dissemination of scientific research documents, whether they are published or not. The documents may come from teaching and research institutions in France or abroad, or from public or private research centers.

L'archive ouverte pluridisciplinaire **HAL**, est destinée au dépôt et à la diffusion de documents scientifiques de niveau recherche, publiés ou non, émanant des établissements d'enseignement et de recherche français ou étrangers, des laboratoires publics ou privés.

SELECTIVE PROPERTIES OF ROUGH SPUTTERED FILMS

G.L. Harding, S. Craig, P. Curmi and M. Lake

Physics School, University of Sydney, N.S.W. 2006 Australia

Abstract.— Solar selective surfaces based on textured copper have been produced by means of two sputtering techniques. In a novel planar magnetron cosputtering system sputter etching of bulk copper sheet, when seeded by a flux of titanium atoms, led to the formation of microscopically roughened surfaces with unusually complex structural formations. Preliminary sputter etching experiments have also been carried out in a cylindrical magnetron system. Alternatively, a standard planar magnetron system was used to deposit copper films of thickness 0.5 μm to 10.0 μm onto glass at sputtering pressures in the range 0.5 Pa to 100 Pa. This deposition technique also resulted in the formation of microscopically roughened surfaces, in this case characterised by arrays of cones. Optical properties of both types of surface follow well defined trends as deposition conditions vary. High absorptance, low emittance selective surfaces have been produced by coating homogeneous metal carbide films onto suitably textured copper on glass films. This composite selective surface exhibits good stability at temperatures up to 500°C in vacuum.

1. **Introduction.**— One method of producing solar selectivity is to create physical roughness of suitable scale on a highly reflecting metal surface. For example dendritic tungsten /1/ and nickel /2/ deposited by CVD exhibit selectivity for dendrite spacings $\sim 1 \mu\text{m}$. Strong absorption occurs for wavelengths smaller than this spacing due to multiple reflections among the dendrites. The surface appears flat for longer wavelengths, hence has relatively high reflectance and low emissivity. Sputter etching of bulk metal surfaces when seeded by atoms of lower sputtering yield also produces microscopically roughened surface /3-10/. The surface morphologies observed can usually be classified in terms of cone, rod or ridge structures /3,7/. High solar absorptance (α) and low emittance (ϵ) may be obtained for surfaces with structures of suitable characteristic dimensions /3/. High surface temperatures produced by the ion bombardment during sputtering are important in this texturing process to promote surface mobility of the seed material. When the seed is sufficiently mobile, the impurity tends to collect in islands which give rise to the various surface formations as etching proceeds. In sections 2 and 3 of this paper we discuss selective surfaces formed on the surface of bulk metal by sputter etching processes carried out in novel cosputter etching systems. One system allows a copper plate to

be moved in oscillatory fashion through a planar magnetron sputter discharge while exposed to a flux of titanium seed, with resultant microscopic roughening of its surface. Sputter etching is also being studied in a cylindrical magnetron sputtering system suitable for production of selective surfaces on long metal strips and tubes. An alternative method of producing textured metal surfaces is suggested by the work of Thornton /12-14/ who obtained significant variations in surface topography for thick copper films (25-250 μm) sputtered at low argon pressures (0.13 and 3.9 Pa) onto substrates maintained at temperatures in the 20°C to 1000°C range. Thornton suggests that the structures arose from the effects of three growth processes: shadowing by high points on the surface, diffusion of atoms on the surface and recrystallisation and grain growth at the higher temperatures.

In section 4 of this paper we discuss the effects of film thickness and sputter gas pressure on copper coatings deposited onto glass substrates in a planar magnetron sputtering system, with the aim of developing selective surfaces for all glass tubular evacuated collectors. For mass production, rapid deposition of surfaces requires that relatively thin films be deposited, and the difficulty of controlling glass tube temperature makes room temperature deposition preferable. Hence film thicknesses 0.5 - 10 μm deposited on to room temperature glass substrates have been studied for an extended range of argon pressures 0.5 - 100 Pa in the sputtering system.

2. Planar magnetron sputter etching.- The sputtering system is shown schematically in figure 1. A planar magnetron with titanium electrode was used to seed the sample which consisted of copper sheet 50 mm x 80 mm x 1.0 mm. The copper sheet was supported in a frame which could be made to translate to left or right along a horizontal rail by a motor outside the vacuum system. The frame was coupled to the motor via a tapped collar on a threaded rod and a rotary feed through the vacuum chamber wall. An assembly of bar magnets underneath the copper sample established a magnetron sputter zone in the form of a rectangular track (Fig.2.).

No cooling system was employed for the copper sample as high temperatures promote titanium seed migration during sputtering. Measurements showed that during sputtering of the copper, the temperature rose steeply in the first three to five minutes, then levelled off to an equilibrium value depending on the sputtering power (Fig.3). For the same sputtering power, the equilibrium temperatures reached varied by $\pm 50^\circ\text{C}$ for the samples studied due to variations in emittance of the etched surface for the different specimens.

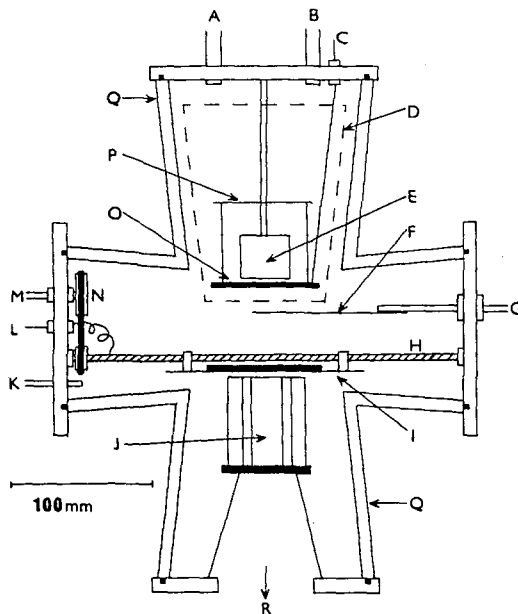


Fig.1.- Sectional view of the planar magnetron co-sputter etching system: (A) Pirani pressure gauge ; (B) Penning pressure gauge ; (C) High voltage feedthrough for titanium seed electrode ; (D) grounded copper shield surrounding the titanium electrode assembly ; (E) 'pot' magnet for titanium planar magnetron ; (F) Grounded shutter ; (G) Linear feedthrough for shutter translation ; (H) Threaded drive shaft ; (I) Copper sample in sample holder attached to threaded shaft ; (J) Magnet assembly for copper magnetron ; (K) Argon inlet ; (L) High voltage feedthrough for copper sample ; (M) Rotary feedthrough coupling d.c. motor to pulley system ; (N) Belt and pulley system coupling shaft to feedthrough ; (O) Titanium target ; (P) Insulating mica support for target ; (Q) Glass vacuum chamber ; (R) Pumping port.

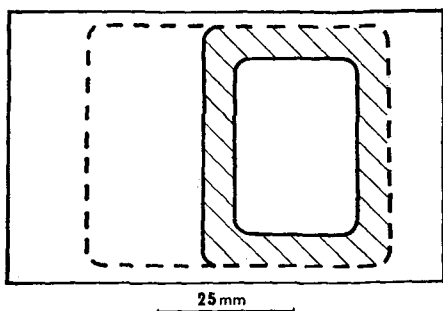


Fig.2.- Copper sample showing the region of plasma bombardment for stationary sample (hatched) and the region etched during continuous oscillatory co-sputter etching (enclosed in broken line).

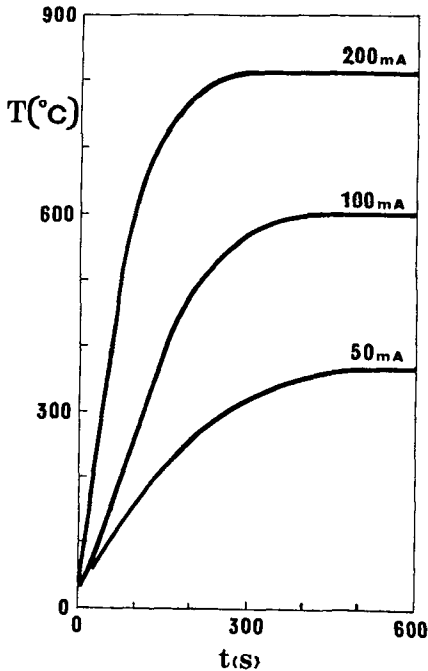


Fig.3.- Typical curves of copper sample temperature (T) vs. sputtering time (t) for various etching currents. Variations in temperature of $\pm 50^\circ\text{C}$ were observed for the plateaux.

A procedure was developed empirically for production of acceptable selective surfaces on stationary copper samples /11/. The procedure involved sputtering the copper at 200 mA for 120s to preheat it to $\sim 700^\circ\text{C}$ in the absence of titanium seed, secondly the copper was coated with ~ 30 nm of titanium in 60 s. Finally the copper electrode was sputtered at 200 mA for 60-90s while titanium was deposited at ~ 0.50 nms^{-1} . Argon at pressure 3.0 Pa was used in all sputtering processes. It is in the final stage that the etching occurred and selective surfaces with $\alpha = 0.90 \pm 0.04$ and room temperature emittance $\varepsilon = 0.11 \pm 0.03$ were produced in the ~ 6 mm wide sputter zone (Fig.2).

Reflectance of a typical surface with $\alpha \sim 0.92$, and $\varepsilon \sim 0.08$ is shown in figure 4. The topography of surfaces textured in these experiments resembled coiled ridges (Fig.5a). Similar structures have been observed by other workers /7, 9/. Regions of discrete needles were sometimes interspersed among the ridges (Fig.5b).

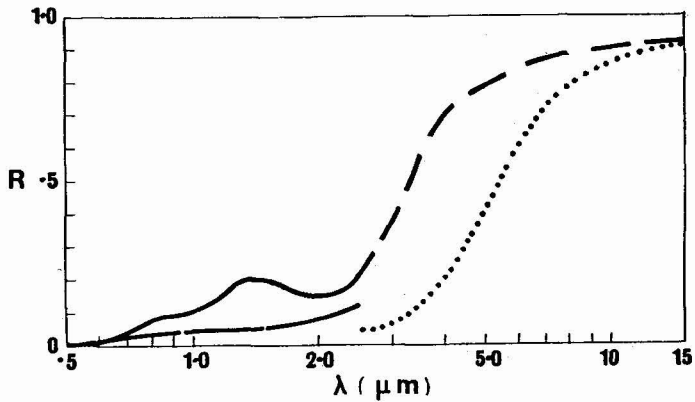


Fig. 4.- Reflectance (R) vs. wavelength (λ) for two textured copper samples. Solid line : total reflectance, short dashed line : specular reflectance for a stationary sample treated with a titanium deposition rate of 0.50 nm.s^{-1} for a 60s time exposure in the final step. $\alpha = 0.92$, $\epsilon = 0.08$ for this specimen. Long dashed line : total reflectance, dotted line ; specular reflectance for a mobile sample treated with a titanium deposition rate of 0.38 nm.s^{-1} in the final step. $\alpha = 0.95$, $\epsilon = 0.20$ for this specimen.

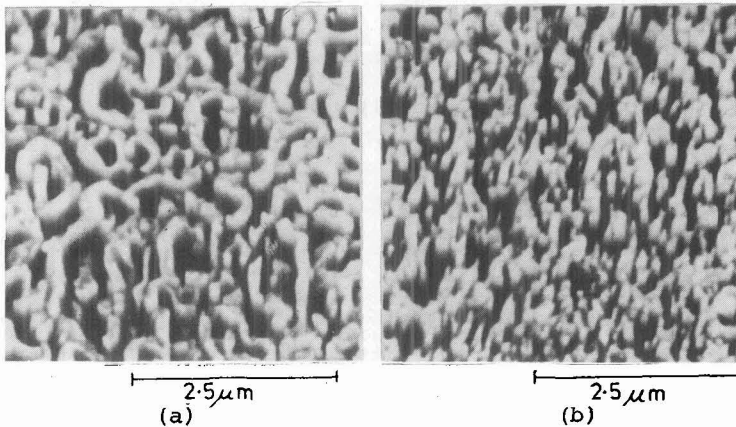


Fig.5.- Electron micrographs showing surface morphology for stationary sputter etched samples. (a) Coiled ridges. (b) Needles occasionally interspersed among ridges.

Translation of the specimen in oscillatory fashion has been used to produce uniform areas of selective surface in a region $50 \text{ mm} \times 45 \text{ mm}$ (Fig. 2). A procedure similar to that for stationary specimens was used, how-

ever in the final (sputter etching) stage, a sputtering time of 300s and various titanium deposition rates (0.14 nms^{-1} to 0.50 nms^{-1}) were used. Good selective properties were obtained, higher α and ϵ values being associated with the higher titanium seed deposition rates. Figure 4 shows the reflectance for a specimen with $\alpha = 0.95$ and $\epsilon = 0.20$, produced using a titanium deposition rate of 0.38 nms^{-1} . Electron micrographs of this surface (Fig.6) show an unusually complex ridge structure.

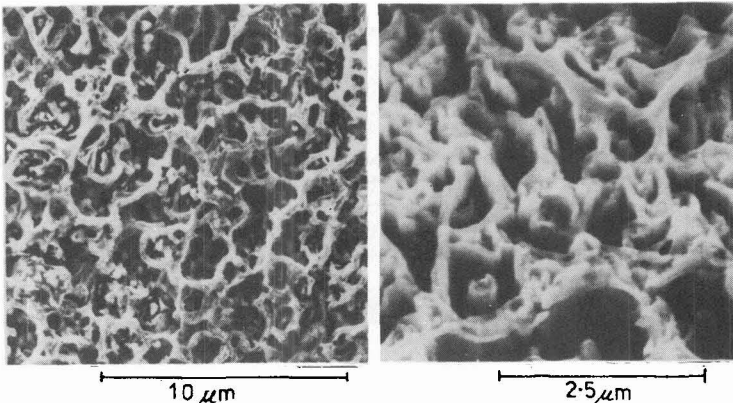


Fig.6.- Electron micrographs showing surface morphology for a sample translated through the sputter discharge with titanium deposition rate 0.38 nm.s^{-1} .

A simplified etching procedure involved translating the sample in oscillatory fashion, sputtering it continuously at 200 mA and continuously depositing seed at 0.38 nms^{-1} , 0.44 nms^{-1} or 0.50 nms^{-1} . Etching times were varied between 5 and 12 minutes.

The selective surfaces produced were not perfectly reproducible, however some trends in α and ϵ are clear. Figure 7 shows α and ϵ for titanium deposition rates 0.38 , 0.44 and 0.50 nms^{-1} , as a function of total sputtering time. The highest titanium deposition rates resulted in highest emittance (except for a few anomalous specimens). Optimum selectivity was obtained for the 0.44 nms^{-1} rate. Figure 8 shows reflectance vs wavelength for two specimens. A wide range of surface morphologies was obtained for this production technique /11/.

Samples of sputter etched surface were enclosed in a continuously pumped vacuum chamber and subjected to a temperature of 500°C for $> 4,000$ hours. Figure 9 shows α and ϵ vs annealing time for a specimen of initial absorptance 0.95 and initial emittance 0.20 . Both α and ϵ decrease for the first $2,000$ hours, then appear to become stable. The final ab-

sorptance is $\alpha \sim 0.88$ and final emittance ~ 0.09 . It is not clear whether the structure of the surface changes during annealing at this temperature. A possible mechanism for the changes is slow oxidation of residual titanium on the surface due to extremely low partial pressures of oxygen or H_2O in the vacuum chamber.

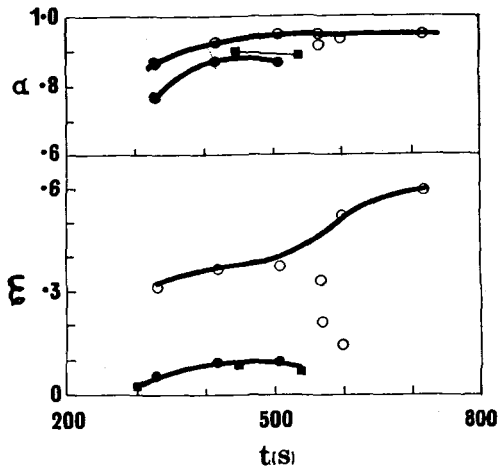


Fig.7.- Absorptance (α) and emittance (ϵ) vs.co-sputtering time (t) for various titanium seed deposition rates. Samples were etched by the continuous co-sputter etching procedure. Solid circles : 0.38 nm.s^{-1} ; solid squares : 0.44 nm.s^{-1} ; open circles : 0.50 nm.s^{-1} .

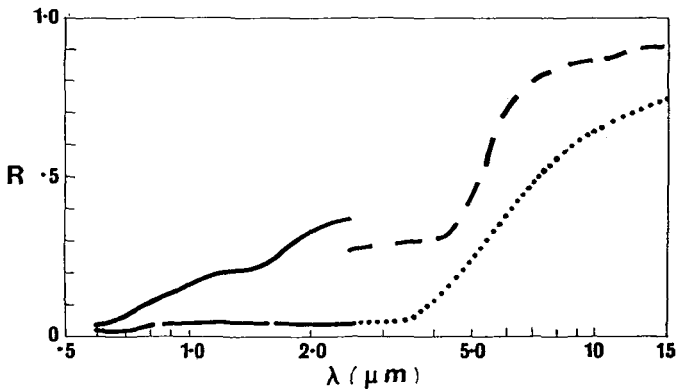


Fig.8.- Reflectance (R) vs.wavelength (λ) for samples produced by the continuous co-sputter etching procedure. Solid line : total reflectance, short dashed line : specular reflectance for titanium deposition rate 0.44 nm.s^{-1} , total sputtering time 7.5. min. $\alpha = 0.90$, $\epsilon = 0.11$ for this specimen. Long dashed line: total reflectance, dotted line : specular reflectance for titanium deposition rate 0.50 nm.s^{-1} , total sputtering time 7 min. $\alpha = 0.93$, $\epsilon = 0.37$ for this specimen.

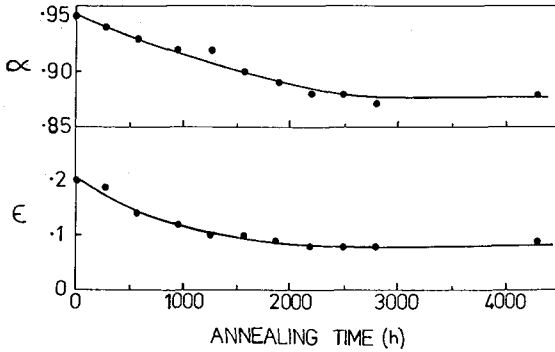


Fig.9.- Absorptance (α) and emittance (ϵ) vs. ageing time for a sputter etched copper surface annealed in vacuum at 500°C.

3. Sputter etching in a cylindrical magnetron.- Sputter etching experiments are now being carried out in a cylindrical magnetron sputtering system suitable for production of selective surfaces on long metal plates and metal tubes. Figure 10 shows a schematic diagram of the coating system.

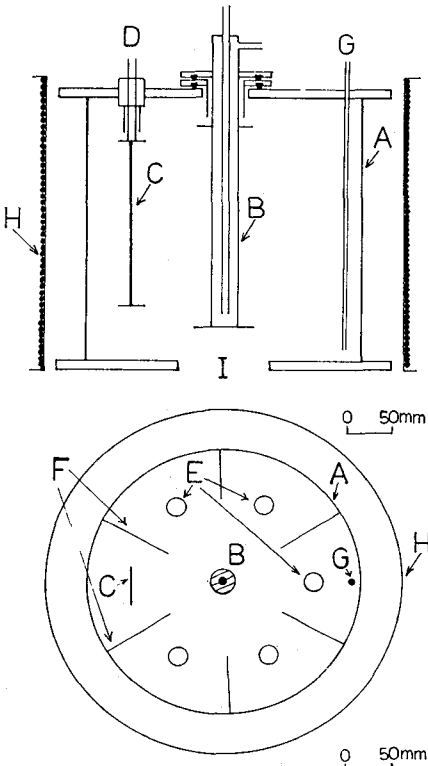


Fig.10.- Sectional view of a cylindrical magnetron sputter etching system. A : Vacuum chamber ; B : Titanium electrode ; C : Metal plate for sputter etching ; D : Rotary feedthrough (and high voltage feedthrough) ; E : Metal tubes for sputter etching ; F : Screens to minimize cross contamination of sputter etched specimens ; G : Argon inlet ; H : magnet coil.

A central titanium electrode provides seed material for metal plates or tubes. The titanium electrode is water cooled, however the sputtered plates or tubes lose energy only by radiation and thermal conduction through the argon gas and so reach high temperatures. Six or more plates or tubes could in principle be sputter etched simultaneously using the chamber design shown. Rotary feedthroughs allow the specimens to be rotated during etching. The sputter etching of copper strips, 260 mm x 50 mm x 0.6 mm is presently being investigated.

Selective surfaces with $\alpha \sim 0.90$ and $\epsilon \sim 0.10$ have been produced with excellent uniformity along the strip. Sputtering time, seed deposition rate and sputter gas pressure are being varied in an attempt to optimise the selective surface manufacture. The etching of alternative materials such as stainless steel and nickel will also be investigated.

4. Sputtered copper films on glass substrates.- A planar magnetron was used as a high rate sputtering source to deposit copper coatings onto glass substrates at room temperature (Fig.11).

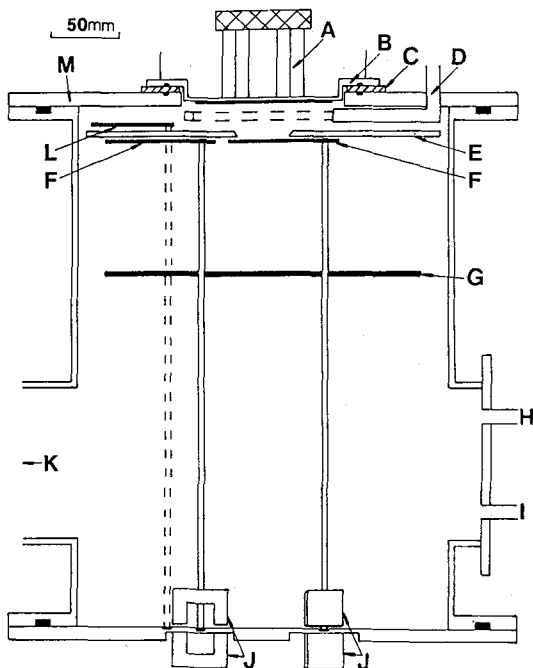


Fig.11.- Sectional view of planar magnetron sputter coating system. A : Permanent magnet array ; B : Cathode assembly ; C : Teflon insulator ; D : Argon inlet ; E : Anode with central aperture ; F : Rotating substrate mount ; G : Guide for drive shafts of substrate mounts and shutter ; H, I : Pressure gauges ; J : Magnetically coupled feedthrough for substrate mounts ; K : Pumping port ; L : Shutter ; M : Grounded vacuum chamber.

Six glass substrates were thermally clamped to two grounded rotating copper platforms, enabling the substrates to be held at room temperature while individually exposed to the sputtered flux through an aperture

in the anode. The chamber was initially evacuated to a base pressure of < 0.1 mPa using a four inch liquid nitrogen trapped oil diffusion pump. Deposition parameters for the sputtered copper films are listed in table I. Deposition rate, argon gas flow rate, glass substrate temperature and electrode-substrate distance were effectively constant for all films. Argon pressure was regulated by throttling the diffusion pump, and measured using a Pirani gauge calibrated within 2%. Different film thicknesses were obtained by varying the exposure time of the glass substrates to the sputtered flux.

Table I.- Deposition conditions for copper films deposited onto glass substrates.

Cathode	OFHC Copper						
Magnetic field	0.080 T						
Target-substrate distance	25 mm						
Substrate temperature	(300 ± 15) K						
Deposition rate	0.5 $\mu\text{m}/\text{min}$.						
Film thickness ($\pm 10\%$) (μm)	0.5	1.0	3.0	10			
Deposition time (min)	1.0	2.0	6.0	20.0			
Argon gas flow rate	$2.7 \times 10^{-7} \text{ m}^3 \text{ s}^{-1}$ at STP						
Argon pressure (Pa)	0.65	6.5	19.5	39	65	97.5	
Discharge Current (A)	0.45	0.65	1.0	1.6	2.4	3.4	
Current density (Am^{-2})	280	410	630	1,000	1,500	2,200	
Discharge voltage (V)	405	355	340	340	345	355	

The basic surface topographical features observed were arrays of cones. Figure 12 shows scanning electron micrographs viewed at 25° to the plane of the surfaces. The micrographs illustrate the trend in surface features as sputtering pressure and film thickness is varied. The surface density of cones increases with sputtering pressure, ranging from the relatively featureless surfaces of films sputtered at low argon pressures to the densely packed cones of high pressure deposited films. Cone size is proportional to film thickness, having dimensions of order 10% of the thickness. For film thickness $3 \mu\text{m}$ and $10 \mu\text{m}$, as argon pressures increase from 20 Pa to 100 Pa, cone size decreases corresponding to a transition from isolated clusters of cones to a densely packed array.

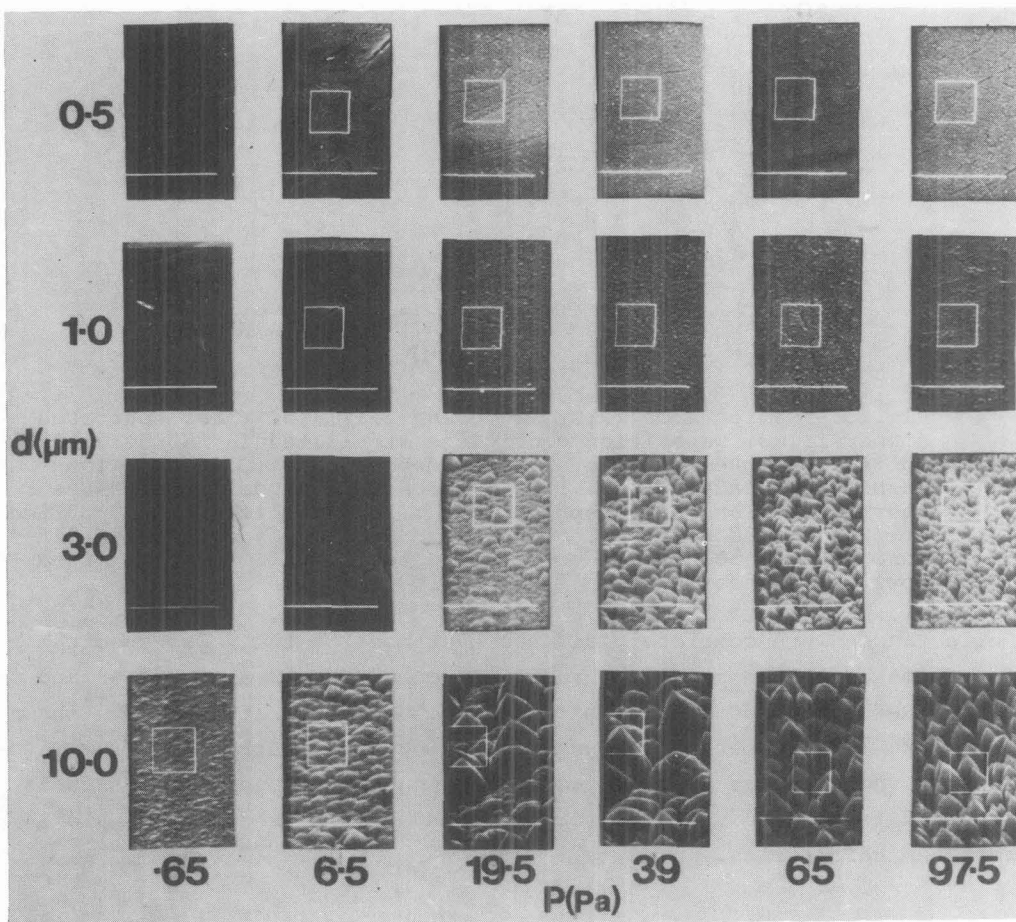


Fig.12.- Scanning electron micrographs viewed at 25° to the film surface showing surface morphology for films of various thicknesses (d) deposited at various argon pressures (P). Magnification is the same for each micrograph, the squares having side $1.5 \mu\text{m}$.

The optical properties of the copper films displayed a marked dependence on the surface morphology. Independent of thickness, films sputtered at 0.65 Pa were specular, with reflectance in the visible and infra-red within a few percent of polished bulk copper (Fig.13). For films of thickness 0.5 to $1.0 \mu\text{m}$, the diffuse component of total reflectance was negligible and total reflectances decreased with increasing pressure for wavelengths in the solar spectrum. Figure 13 shows reflectance vs wavelength for a $1 \mu\text{m}$ thick film deposited at 39 Pa . For films of thickness $3.0 \mu\text{m}$ and $10.0 \mu\text{m}$, the diffuse component of the total reflectance was significant and increased with pressure, corresponding with increa-

sing density of cones of characteristic dimensions 0.3 to 1.0 μm .

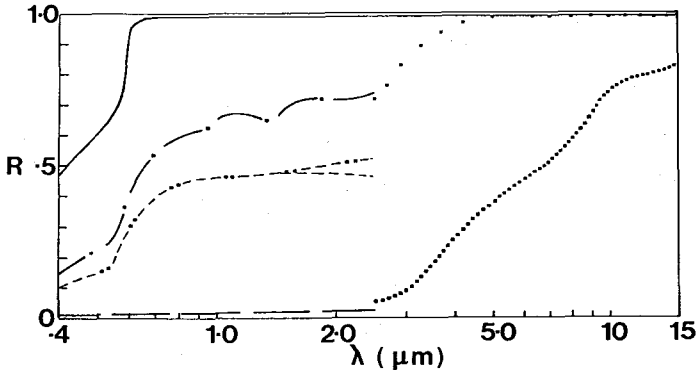


Fig.13.- Reflectance (R) vs. wavelength (λ) for three sputtered copper films. Deposition conditions are listed in table I. Solid line : Reflectance of films deposited at 0.65 Pa ; long dashes and spaced dots : 1.0 μm thick film deposited at 39 Pa ; Short dashes and close spaced dots : 10 μm thick film deposited at 39 Pa. (Specular reflectance is indicated by dots only, diffuse reflectance by dashes only and total reflectance by mixed dots and dashes).

Reflectances were completely diffuse over most of the solar spectrum for films of thickness 3.0 μm and 10.0 μm manufactured at 39, 65 and 97 Pa. Reflectances of a 10 μm thick film deposited at 39 Pa are shown in figure 13. A general trend of decreasing total reflectance for wavelengths in the solar spectrum as sputtering gas pressure increases is observed for all four film thicknesses and this is shown in figure 14 for 3 μm thick films.

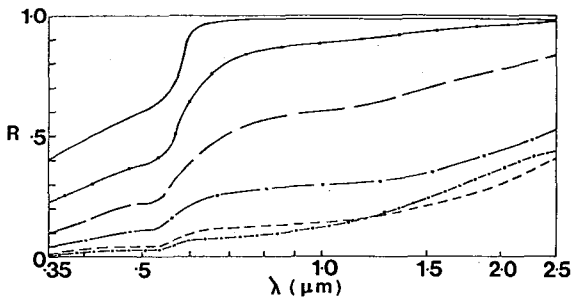


Fig.14.- Total reflectance (R) vs. wavelength (λ) for 3 μm thick sputtered copper films. Deposition conditions are listed in table I. Solid line : film deposited at 0.65 Pa ; Solid line with dots : film deposited at 6.5 Pa ; long dashed line : film deposited at 19.5 Pa ; long dashed line with dots ; film deposited at 39 Pa ; Short dashed line : film deposited at 65 Pa ; Short dashed line with dots : film deposited at 97.5 Pa.

Figures 15 to 18 illustrate the trends in absorptance α and room temperature emittance ϵ for varying film thickness and sputtering pressure. Absorptance and emittance increase with film thickness and sputtering pressure. Most absorptances and emittances were reproducible within a few percent.

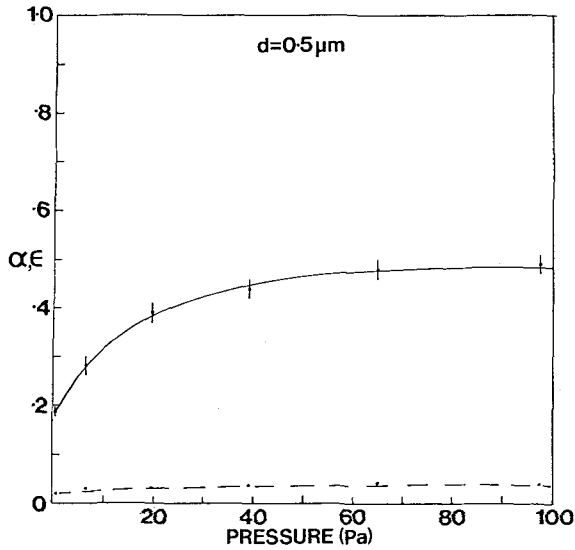


Fig.15.- Absorptance (α) and emittance (ϵ) at 300K vs. sputtering gas pressure for copper film thickness $0.5\ \mu\text{m}$.

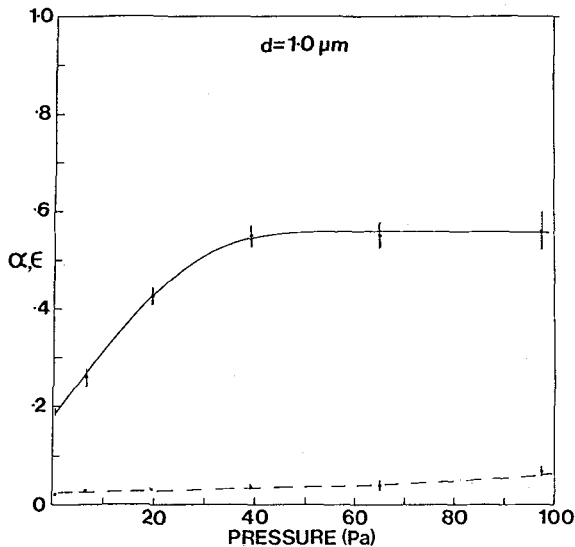


Fig.16.- Absorptance (α) and emittance (ϵ) at 300K vs. sputtering gas pressure for copper film thickness $1.0\ \mu\text{m}$.

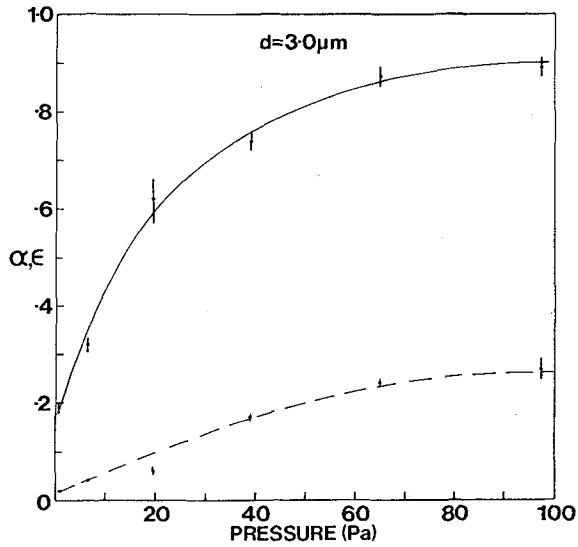


Fig.17.- Absorptance (α) and emittance (ϵ) at 300K vs. sputtering gas pressure for copper film thickness $3.0 \mu\text{m}$.

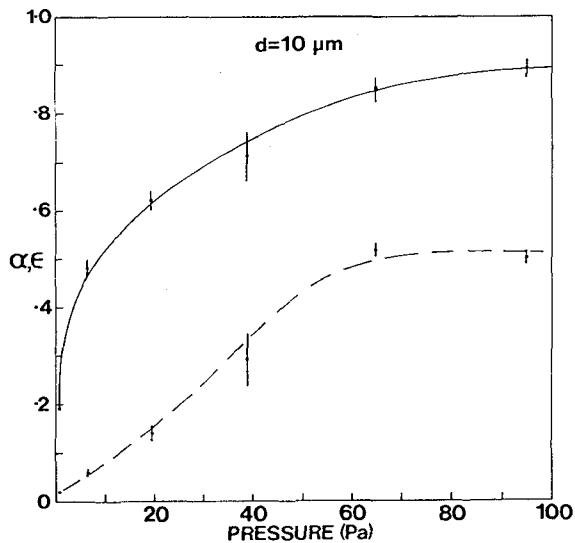


Fig.18.- Absorptance (α) and emittance (ϵ) at 300 K vs. sputtering gas pressure for copper film thickness $10.0 \mu\text{m}$.

Optimum values of α/ϵ are obtained for the $1.0 \mu\text{m}$ thick films deposited at 39 Pa. High solar absorptances and moderately low emittances have

been obtained by coating a reactively sputtered homogeneous metal carbide film on these films.

Absorptances $\alpha \sim 0.90$ and $\epsilon \sim 0.04$ to 0.05 were obtained compared to $\alpha \sim 0.80$ and $\epsilon \sim 0.02$ for a similar interference layer on smooth copper deposited at 0.65 Pa. Figure 19 shows reflectance vs. wavelength for a metal carbide deposited onto smooth and textured films. The latter films have been aged at 200°C , 300°C , 400°C and 500°C in a continuously pumped vacuum chamber at pressure < 1 mPa. Ageing results are summarised in table II.

Table II.- Solar absorptance α and emittance ϵ (at 300K) before and after ageing for homogeneous stainless steel carbide films on textured copper.

Ageing Temperature		200°C				
Total time (h)	0	200	1000	1500	2000	3500
α	0.895	0.86	0.85	0.845	0.845	0.845
ϵ	0.053	0.042	0.040	0.044	0.043	0.042
Ageing Temperature		300°C				
Total time (h)	0	200	1000	1500	2000	3500
α	0.90	0.89	0.89	0.895	0.895	0.895
ϵ	0.054	0.034	0.034	0.035	0.034	0.035
Ageing Temperature		400°C				
Total time (h)	0	200	1000	1500	2000	3500
α	0.90	0.89	0.895	0.90	0.90	0.90
ϵ	0.052	0.035	0.036	0.037	0.037	0.037
Ageing Temperature		500°C				
Total time (h)	0	300	600	2000		
α	0.90	0.92	0.92	0.94		
ϵ	0.035	0.042	0.042	0.047		

The absorptances are stable at 300°C and 400°C while emittances decrease initially. At 500°C both absorptance and emittance increase slowly possibly due to diffusion at the metal carbide-copper interface /16/. The anomalous decrease in absorptance during the 200°C anneal may be associated with reaction of the metal carbide surface with residual gas in the continuously pumped chamber.

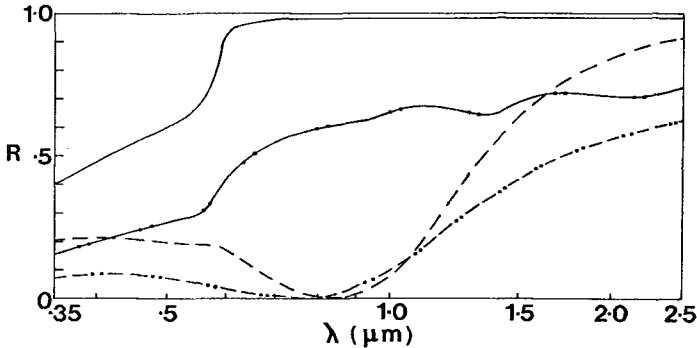


Fig.19.- Reflectance (R) vs. wavelength (λ) for homogeneous metal carbide layers overlayed on copper films sputtered at 0.65 Pa (smooth surfaces) and 39 Pa (textured surfaces). Solid line : Copper deposited at 0.65 Pa ; solid line with dots ; Copper deposited at 39 Pa ; Dashed line : Metal carbide overlayed on 0.65 Pa copper ; Dashed line with dots : Metal carbide overlayed on 39 Pa copper.

5. Conclusion.- Sputter etching of copper using a planar magnetron system yielded good selective surfaces with moderate stability at 500°C. However this etching apparatus does not seem easily adaptable to producing large areas of selective surface.

The cylindrical magnetron technology offers greater prospects in this regard, however work at Sydney University is still in a preliminary stage. Sputter etched strip or pipe may form a suitable receiver element in vacuum insulated glass envelopes incorporated in parabolic trough concentrators or CPCs designed for production of high temperatures (300 - 500°C). Alternative materials to copper such as stainless steel and nickel may offer greater stability at high temperatures in vacuum or in air. Coating of these surfaces with a refractory material may also improve the stability of the surface.

Selective surfaces based on textured thin copper films deposited on glass in high argon pressures offer an interesting prospect for all-glass evacuated collectors. However, as the mechanism of formation of these surfaces is unclear, it is not known whether mass production of the textured films is feasible.

Acknowledgements.- The authors would like to thank their colleagues Dr. C. M. Horwitz, Dr. R. McPhedran and Dr. D. McKenzie for advice and encouragement. This work was funded by grants from the Sydney University Energy Research Centre, the Government of New South Wales and Saudi Arabian interests under the auspices of the University of Sydney Science Foundation.

References

- /1/ Cuomo, J.J., Ziegler, J.F. and Woodwall, J.M., Appl. Phys. Lett. 26 (1975) 557
- /2/ Grimmer, D.P., Hern, K.C. and McCreary, W.J., J. Vac. Sci. Technol. 15 (1978) 59
- /3/ Berg, R.S. and Kominiak, G.J., J. Vac. Sci. Technol. 13 (1975) 403
- /4/ Witcombe, M.J., J. Appl. Phys. 46 (1975) 5053
- /5/ Vossen, J.L., J. Phys. E. 12 (1979) 159
- /6/ Wehner, G.K. and Hajicek, D.J., J. Appl. Phys. 42 (1971) 1145
- /7/ Hudson, W.R., J. Vac. Sci. Technol. 30 (1977) 286
- /8/ Wehner, G., J. Appl. Phys. 30 (1959) 1762
- /9/ Oohashi, T. and Yamanka, S., Japan J. Appl. Phys. 11 (1972) 1581
- /10/ Stewart, A.D.G. and Thompson, M.W., J. Mater. Sci. 4 (1969) 56
- /11/ Curmi, P. and Harding, G.L., To be published in J. Vac. Sci. Technol. (Nov. 1980).
- /12/ Thornton, J.A., J. Vac. Sci. Technol. 11 (1974) 666
- /13/ Thornton, J.A., J. Vac. Sci. Technol. 12 (1975) 830
- /14/ Thornton, J.A., Proc. A.E.S. Coatings for Solar Collectors Symposium. Atlanta, Georgia (1976) 63
- /15/ Harding, G.L. and Craig, S., J. Vac. Sci. Technol. 16 (1979) 857
- /16/ Harding, G.L., Sol. Energy Materials. 2 (1980) 469